

# Optomechanical cooling of levitated spheres with doubly-resonant fields

G A T Pender,<sup>1</sup> P F Barker,<sup>1</sup> Florian Marquardt,<sup>2</sup> James Millen,<sup>1</sup> and T S Monteiro<sup>1</sup>

<sup>1</sup>*Department of Physics and Astronomy, University College London,  
Gower Street, London WC1E 6BT, United Kingdom*

<sup>2</sup>*Institut for Theoretical Physics, Universität Erlangen-Nürnberg, Staudtstraße 7, 91058 Erlangen Germany*

Optomechanical cooling of levitated dielectric particles represents a promising new approach in the quest to cool small mechanical resonators towards their quantum ground state. We investigate two-mode cooling of levitated nanospheres in a self-trapping regime. We identify a rich structure of split sidebands (by a mechanism unrelated to usual strong-coupling effects) and strong cooling even when one mode is blue detuned. We show the best regimes occur when both optical fields cooperatively cool and trap the nanosphere, where cooling rates are over an order of magnitude faster compared to corresponding single-sideband cooling rates.

PACS numbers:

Extraordinary progress has been made in the last half-dozen years [1, 2] towards the final goal of cooling a small mechanical resonator down to its quantum ground state and hence to realise quantum behavior in a macroscopic system. Implementations include cavity cooling of micromirrors on cantilevers [3–6], dielectric membranes in Fabry Perot cavities [7]; radial and whispering gallery modes of optical microcavities [8] and nanoelectromechanical systems [9]. Indeed the realizations span 12 orders of magnitude [2], up to and including the LIGO gravity wave experiments. Corresponding advances in the theory of optomechanical cooling have also been made [10–13].

Over the last year or so, a promising new paradigm has been attracting much interest: several groups [14–17] have now proposed schemes for optomechanical cooling of levitated dielectric particles, including nanospheres and even viruses [14]. The important advantage is the elimination of the mechanical support, a dominant source of heating noise. In general, these proposals involve two fields, one for trapping and one for cooling. This may involve an optical cavity mode plus a separate trap; or two optical cavity modes, the so-called “self-trapping” scenario.

Mechanical oscillators in the self-trapping regime differ from other optomechanically-cooled devices in a second fundamental respect (in addition to the absence of mechanical support): the mechanical frequency,  $\omega_M$ , associated with centre of mass oscillations is not an intrinsic feature of the resonator but is determined by the optical field. In particular, it is a function of one or both of the detuning frequencies,  $\delta_1$  and  $\delta_2$ , of the optical modes. Cooling, in general, occurs when  $\omega_M$  is resonantly red detuned with either of the detuning frequencies (i.e. negative  $\delta_{1,2}$  is associated with cooling). For self-trapping systems, this means  $\omega_M(\delta_1, \delta_2) \sim -\delta_{1,2}$  so the relevant frequencies are not independent.

The full implications of this nonlinear interdependence of the resonant frequencies have not yet been fully elucidated. We show here for the first time that it leads to a rich landscape of split sidebands. The mechanism here is unrelated to splittings seen in experiments in the

strong-coupling regime [19]. However, it results in extremely favourable cooling regimes, where two (or more) cooling sidebands approach each other. We term this the “double-resonance” regime. We find it can produce cooling rates nearly two orders of magnitude stronger than the corresponding “single-resonance” case. A self-

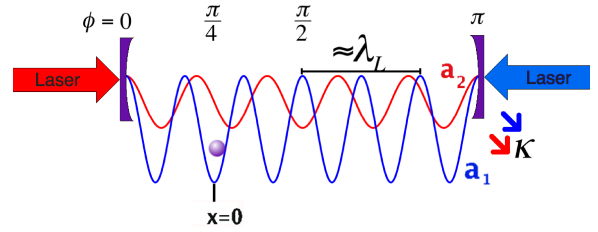


FIG. 1: Schematic set-up: a levitated nanosphere is trapped and cooled cooperatively by two optical modes. The optical potential for each mode is shown.

trapping Hamiltonian was investigated in [15] and corresponds to the set-up illustrated in Fig.1:

$$\begin{aligned} \hat{H} = & -\delta_1 \hat{a}_1^\dagger \hat{a}_1 - \delta_2 \hat{a}_2^\dagger \hat{a}_2 + \frac{\hat{P}^2}{2m} - A \hat{a}_2^\dagger \hat{a}_2 \cos^2(k_2 x - \phi) \\ & - A \hat{a}_1^\dagger \hat{a}_1 \cos^2 k_1 x + E_1 (\hat{a}_1^\dagger + \hat{a}_1) + R E_1 (\hat{a}_2^\dagger + \hat{a}_2) \end{aligned} \quad (1)$$

Two optical field modes  $\hat{a}_{1,2}$  are coupled to a nanosphere with centre of mass position  $x$ .  $\hat{H}$  is given in the rotating frame of the laser which drives the modes with amplitudes  $E_1$  and  $R E_1$  respectively. In [15], the phase between the optical potentials was chosen to be  $\phi = \pi/4$ ; the study focussed primarily on the  $\delta_1 \simeq 0$  regime, where the  $\hat{a}_1$  mode is responsible exclusively for trapping while the  $\hat{a}_2$  mode alone provides cooling. Previous studies [14, 15, 17] all analysed mechanical oscillations about an equilibrium position  $x_0 \simeq 0$ , corresponding to the antinode of the trapping mode (field 1). Below, this scenario is referred to as the “single-resonance” regime.

Here we investigate the effects of relaxing all these restrictions and find interesting and unexpected implications. We take  $\phi = \pi/4$ ; the cooling field is driven

more weakly than the trapping field, but with a ratio  $R \simeq 0.1 - 1$ . Below, our analytical expressions cover arbitrary  $\kappa, R, E_1, A$ , but we compare with an illustrative set of *experimentally plausible parameters*: we take a cavity damping  $\kappa = 6 \times 10^5 \text{ Hz}$ . We considered driving powers in the range  $P \simeq 1 - 10 \text{ mW}$ , where  $P = \frac{2\kappa c E_1^2 \hbar}{\kappa}$ . For a laser of wavelength  $\lambda = 1064 \text{ nm}$  and a cavity of length  $L \sim 1 \text{ cm}$ , waist  $25 \mu\text{m}$  we consider a silica nanosphere of  $100 \text{ nm}$  radius and hence a coupling strength  $A \simeq 3 \times 10^5 \text{ Hz}$ . To obtain a dephasing of  $\pi/4$  between the two modes near the centre of the cavity, the frequency difference between the modes is  $|\omega_1 - \omega_2| \sim 2\pi \times 10 \text{ GHz}$ . This far exceeds the detunings  $\delta_{1,2} \sim 1 \text{ MHz}$  and also the mechanical frequencies  $\omega_M$ . Thus the photons are completely distinguishable and can be read out and driven separately. Nevertheless, since  $\omega_{1,2} \sim 10^{14} \text{ Hz}$ , we approximate  $k_1 \simeq k_2 \equiv k$ . However, this situation is distinct from the ring-cavity proposal of [17] where  $R = 0$  and mode 2 is undriven but is populated exclusively by scattering from mode 1; there, the photons are of precisely the same frequency and thus there is a single detuning parameter involved.

Fig.2 illustrates the behavior for  $R = 0.5$ . It shows that allowing both fields to cooperatively trap and cool yields more than an additive improvement. We denote by  $r2$  and  $r1$  the set of detunings corresponding to cooling resonances of modes 1 and 2 respectively: Fig.2 shows that these resonances unexpectedly split and separate into new cooling resonances  $r1\pm$  and  $r2\pm$ . These can overlap, to give very strong cooling associated with multiple resonances. Below, we also show that the usually studied single-field resonance regime  $r2$  can attain only a maximal cooling rate  $\Gamma \simeq \frac{R^2 A}{4}$ ; and that for strong driving,  $\Gamma \propto 1/E_1$ : thus, the cooling falls with increasing driving and it is hard to achieve optimal cooling regimes where  $\Gamma \simeq A \sim \kappa$ . For the double-field resonances, in contrast,  $\Gamma \propto E_1^{1/2}$ , the cooling increases with  $E_1$  and can more easily reach optimal cooling. Very strong cooling is apparent even for regimes where one mode is blue detuned. In addition, although there is no direct coupling between optical modes, double-resonances offer the prospect of strong (albeit second-order) coupling and entangling of the two modes via the nanosphere, within a single cavity. This includes simultaneous resonant/antiresonant regimes (indicated by the crossing of  $r2+$  and  $a1-$  in Fig.2) where one mode resonantly heats, while the other resonantly cools the mechanical mode.

The dynamics depends on  $k, m, A, \kappa, \delta_1, \delta_2, E_1, R$ . However transforming to scaled variables reduces this complexity. We rescale position, time and field variables as follows:  $kx \rightarrow \tilde{x}$ ,  $At \rightarrow \tilde{t}$ , then  $a_{1,2} \rightarrow \frac{E_1}{iA} \tilde{a}_{1,2}$ . Note that below we drop all the tildes but it is implicit that all variables are scaled in the resulting Heisenberg equa-

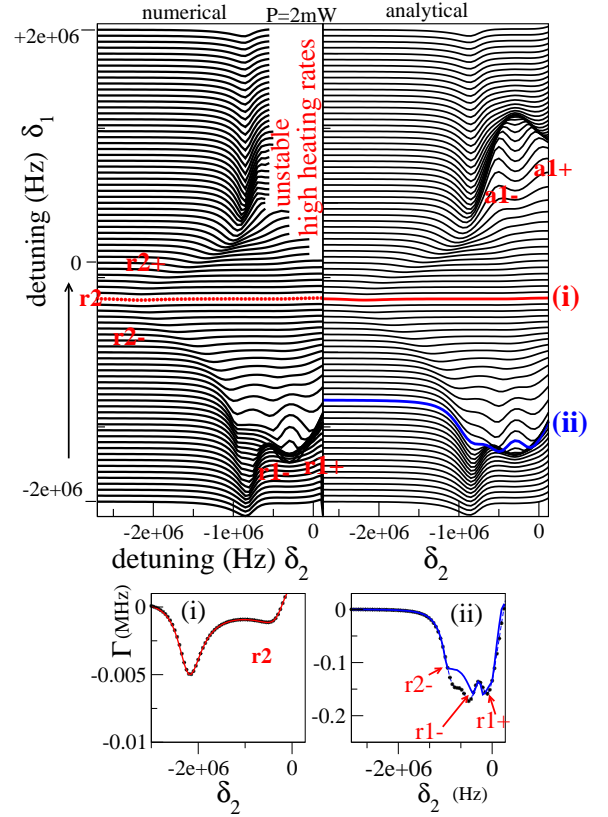


FIG. 2: (Colour online) **Upper Panels:** comparison between numerical optical cooling rates (without linearisation) and an analytical expression (Eq.5) from linearised dynamics, showing excellent agreement.  $R = 0.5$ . The curves corresponding to different values of  $\delta_1 \pm 2 \text{ MHz}$  are shifted relative to each other. At single-resonance  $r2$ , field 2 is resonant with the oscillator and is exclusively responsible for cooling; field 1 is resonant with the cavity ( $\Delta_1^x = 0$ ) and traps the sphere. Subsequently  $r2\pm$  appear: they are cooling resonances of field 1, split by field 2.  $r2-, r1-, r1+$  overlap giving a broad region of very strong cooling. The  $a1\pm$  are heating (Stokes) resonances of field 1. The  $a1-$  can coincide with the cooling resonance ( $r2+$ ). Here field 2 absorbs phonons as fast as field 1 emits them. **Lower Panels:** Show the unshifted cooling curves at the single-field cooling resonance  $r2$  and double-resonant cooling, showing that the latter gives over an order of magnitude stronger cooling. Asterisks are numerical results, blue and red curves correspond to curves in upper panels.

tions:

$$\begin{aligned} \ddot{\tilde{x}} &= -\epsilon^2 [|\hat{a}_1|^2 \sin 2x + |\hat{a}_2|^2 \sin(2x - \pi/2)] \\ \dot{\hat{a}}_1 &= i\Delta_1 \hat{a}_1 + 1 + i\hat{a}_1 \cos^2 x - \kappa_A \hat{a}_1 \\ \dot{\hat{a}}_2 &= i\Delta_2 \hat{a}_2 + R + i\hat{a}_2 \cos^2(x - \pi/4) - \kappa_A \hat{a}_2. \end{aligned} \quad (2)$$

The dynamics for a given  $R < 1$  depends only on the scaled driving  $\epsilon^2 = \zeta E_1^2$  where  $\zeta = \frac{\hbar k^2}{m A^3}$ , two scaled detunings  $\Delta_{1,2} = \delta_{1,2}/A$  and a scaled damping  $\kappa_A =$

$(\kappa/2)$ ; all scaled frequencies (including cooling rates) are given below as a fraction of  $A$ .

The experimentally adjustable parameters are  $\epsilon$ , both the detunings  $\Delta_{1,2}$  and  $R$ . We assume  $\kappa_A \simeq 1$ , though the analytical expressions are for arbitrary  $\kappa_A$ . Varying driving power  $\mathcal{P} \sim 1 - 10$  mW, but leaving the cavity/nanosphere properties unchanged means  $A$  remains constant, but  $\epsilon^2$  varies from  $\sim 1 - 100$ .

Following the usual procedure, we replace operators by their expectation values and linearise about equilibrium fields by performing the shifts  $a_1 \rightarrow \alpha_1 + a_1$ ,  $a_2 \rightarrow \alpha_2 + a_2$  and  $x \rightarrow x_0 + x$ . Hence we find equilibrium photon fields,  $\alpha_1 = [\kappa_A - i\Delta_1^x]^{-1}$  and  $\alpha_2 = R[\kappa_A - i\Delta_2^x]^{-1}$  as well as position  $\tan 2x_0 = |\alpha_2|^2/|\alpha_1|^2$ .

Here,  $\Delta_1^x = \Delta_1 + \frac{1}{2}(1 + \cos 2x_0)$  and  $\Delta_2^x = \Delta_1 + \frac{1}{2}(1 + \sin 2x_0)$ . The dimensionless mechanical frequency is:

$$\omega_M^2(\Delta_1, \Delta_2) = 2\epsilon^2(|\alpha_1|^2 \cos 2x_0 + |\alpha_2|^2 \sin 2x_0). \quad (3)$$

Closely related forms of this ‘‘self-trapping’’ frequency expression have been noted previously [14–17] but the implications, other than for  $x_0 \simeq 0$ , have not been investigated.

To first order, the linearised equations of motion are:

$$\begin{aligned} \ddot{x} &= -\omega_M^2 x - \epsilon^2(g_1 \sin 2x_0 - g_2 \cos 2x_0) \\ \dot{a}_1 &= i\Delta_1^x a_1 - i\alpha_1 x \sin 2x_0 - \kappa_A a_1 \\ \dot{a}_2 &= i\Delta_2^x a_2 + i\alpha_2 x \cos 2x_0 - \kappa_A a_2 \end{aligned} \quad (4)$$

where  $g_i = (\alpha_i^* a_i + \alpha_i a_i^*)$ . From the above, we can obtain the contribution from the two photon fields to the optomechanical cooling:

$$\frac{\Gamma}{2} = \frac{\epsilon^2 \kappa_A}{2\omega_M} [S_1(\omega_M) + S_2(\omega_M) - S_1(-\omega_M) - S_2(-\omega_M)] \quad (5)$$

where

$$S_1(\omega) = \frac{|\alpha_1|^2 \sin^2 2x_0}{[\Delta_1^x - \omega]^2 + \kappa_A^2}; \quad S_2(\omega) = \frac{|\alpha_2|^2 \cos^2 2x_0}{[\Delta_2^x - \omega]^2 + \kappa_A^2} \quad (6)$$

(net cooling occurs for  $\Gamma < 0$ ). We also calculate a numerical  $\Gamma$  by evolving the equations of motion in time and looking at the decay in  $x(t)$  (its variance in particular). The analytical cooling rates give excellent agreement with numerics in all but the strongest cooling regions.

The single-field cooling resonance  $r2$  occurs for  $x_0 \simeq 0$ ,  $\Delta_1^x \simeq 0$  and  $\Delta_2^x = -\omega_M$ , thus here for  $\Delta_1 = -1$  (i.e.  $\delta_1 = -A$ ). Conversely, there is also a single-field cooling resonance  $r1$  for  $x_0 = \pi/4$  (note that since we consider only the case  $R < 1$ , i.e. field 2 is always driven more weakly than field 1, the latter situation does not correspond simply to an interchange in the role of the fields). Away from these extreme cases, both cooling resonances are split by the effect of the other field, wherever  $0 < x_0 < \pi/4$ .

From Fig.2 we see  $r2\pm$  occur for the same  $\Delta_2$ , thus the same equilibrium photon field  $\alpha_2$ ; however they correspond to photon fields  $\alpha_1$  and  $\alpha_1^*$  respectively and thus

to different  $\Delta_1^\pm = \pm y_1$ , where  $2y_1$  is the splitting (about  $\Delta_1^x = 0$ ) between  $r2+$  and  $r2-$  seen in Fig.2.

The transformation  $\alpha_1 \rightarrow \alpha_1^*$  leaves both the mechanical frequency  $\omega_m(\Delta_1^\pm, \Delta_2)$  and  $x_0(\Delta_1^\pm, \Delta_2)$  unchanged. Hence the cooling rates are similar for both  $r2\pm$ .

We can estimate the splitting  $\Delta_1^\pm$  by requiring

$$\omega_M(\Delta_1^+, \Delta_2) = \omega_M(\Delta_1^-, \Delta_2) \simeq \Delta_2^x \quad (7)$$

since  $\omega_M(\Delta_1^\pm, \Delta_2) \simeq \Delta_2^x$  are the conditions for the optomechanical resonance  $r2\pm$ . From Eqs.(16) and (3) we see:

$$\pm y_1 = \pm \sqrt{\frac{2\epsilon^2}{(\Delta_2^x)^2 \cos 2x_0} - \kappa_A^2}. \quad (8)$$

Close to  $r2$ , we can simplify  $y_1 \simeq \pm \frac{\sqrt{2}\epsilon}{\Delta_2 + A/2}$ . Similarly,  $y_2$ , the splitting between  $r1\pm$  is  $\pm y_2 = \pm \sqrt{\frac{2\epsilon^2 R^2}{(\Delta_1^x)^2 \sin 2x_0} - \kappa_A^2}$ .

Thus the splittings increase with driving power and  $R$ . While in Fig.2, corresponding to  $R = 0.5$ , three resonances ( $r2-$ ,  $r1-$  and  $r1+$ ) overlap, in Fig.3, for  $R = 1$   $r1\pm$  are well separated and the double resonance involves only  $r2-, r1-$ .

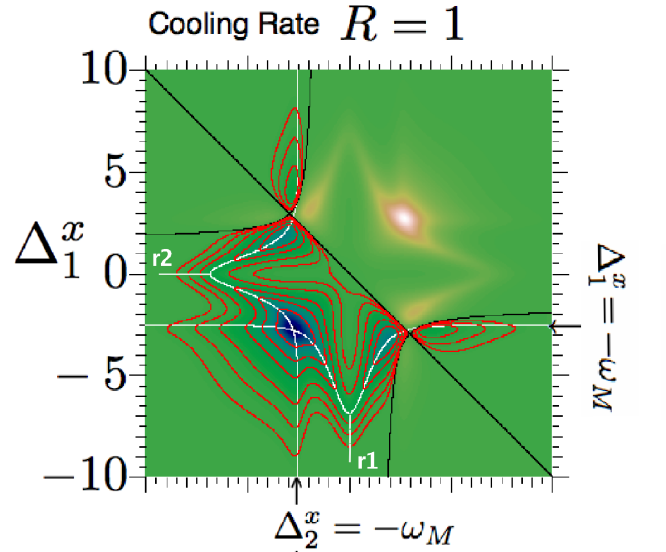


FIG. 3: (Colour online) Cooling rates as a function of scaled detunings. For  $R = 1$  the behaviour of mode 1 and mode 2 is equivalent, thus a high degree of symmetry is evident. The splitting of the resonances is much larger, but very strong cooling maximum (dark blue) at the double-resonance of  $r2-, r1-$  is seen, with a matching heating maximum (white/orange) for  $\Delta_{1,2}^x > 0$ .

We now analyse the relative merits of single-resonance versus double-resonance cooling. Single-field cooling corresponds to  $r2$  in Fig.2. Cooling rates are obtained from Eq.5 by taking  $x_0 \simeq 0$ ,  $\Delta_1^x = 0$  and  $\Delta_2^x = -\omega_M$ . This

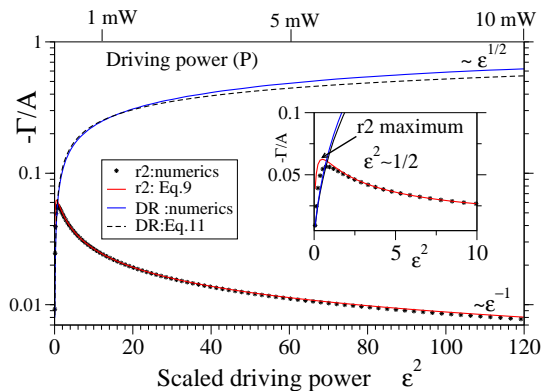


FIG. 4: Comparison between single-resonant ( $r2$ ) and double resonant (DR) i.e. simultaneous  $r1-$  and  $r2-$  resonant cooling rates as a function of laser driving power ( $R = 0.5$ ), showing that the double resonance corresponds to two orders of magnitude greater cooling for strong driving. Inset shows cooling maximum of  $r2$  at weak driving  $\epsilon^2 \simeq 1/2$ ; here the system is on the edge of the sideband-resolved regime  $\omega_M = \kappa_A$ . In contrast for DR, at  $P = 10mW$ ,  $\omega_M/\kappa_A \simeq 4$  and the  $r1-$  and  $r2-$  sidebands are very well resolved.

regime was investigated in [15] and Eq.5 reduces to expressions therein (in unscaled units). However, we can give good approximations to cooling rates purely in terms of experimental parameters (driving power,  $R$  and  $\kappa$ ). Assuming  $S_2(-\omega_M) \gg S_2(+\omega_M)$  and that the field 1 contribution to cooling is negligible, near  $r2$ , the mechanical frequency  $\omega_M^2 = \frac{2\epsilon^2}{\kappa_A^2}$ . Hence, as shown in the appendix, the Single Resonance (SR) cooling rate becomes:

$$-\Gamma_{SR} \approx \frac{R^2 \epsilon \kappa_A^2}{\sqrt{2}} (2\epsilon^2 + \kappa_A^4)^{-1} \quad (9)$$

(recall this is a scaled cooling rate thus given in units of  $A$ ).

Single-field cooling is a maximum if  $\epsilon = \kappa_A^2/\sqrt{2}$  where  $\omega_M = \kappa/2$  (in unscaled units) and is thus at the edge of the resolved sideband regime. Here,  $-\Gamma_{SR} \approx \frac{R^2}{4}$ ; this gives optimal cooling  $\Gamma \sim \kappa$  only if  $R \sim 1$ . This cooling maximum is independent of  $\kappa_A$ : it depends only on  $R$ . As the driving is increased, if  $2\epsilon^2 \gg \kappa_A^4$ ,

$$-\Gamma_{SR} \sim \frac{R^2 \kappa_A^2}{2\sqrt{2}\epsilon} \propto 1/\epsilon \quad (10)$$

Thus the single resonance cooling rate falls off quite

rapidly as the driving amplitude is increased: the cooling cannot be improved by increasing the driving amplitude.

To obtain the corresponding double-resonant rate (DR) one must first identify the  $\epsilon$ -dependent pair of detunings for which  $-\omega_M(\Delta_1, \Delta_2) \approx \Delta_1^x \approx \Delta_2^x$ . Even if  $r1-, r2-$  do not cross in Fig.2, the sidebands approach within their width  $\kappa$  and overlap significantly. One can still obtain a good approximation to the cooling rate in terms of driving parameters (see Appendix). In this case, there are contributions to cooling from both field 1 and field 2. Adding them both,

$$-\Gamma_{DR} \approx \frac{\epsilon^2(R^2 + R^4)}{(\kappa_A \omega_M (\omega_M^2 + \kappa_A^2))} \quad (11)$$

where the frequency is given by the expression,  $\omega_M^2 = \frac{-\kappa_A^2}{2} + \frac{1}{2}\sqrt{\kappa_A^4 + 8\epsilon^2}$ . The contribution from mode  $2 \propto R^2$  while that of mode  $1 \propto R^4$ ; both contribute significantly for  $R \gtrsim 0.5$ . Assuming  $\omega_M \gg \kappa_A$ , this reduces to  $-\Gamma_{DR} \approx 2^{-3/4}(R^2 + R^4)\epsilon^{1/2}/\kappa_A$ , hence  $\Gamma_{DR} \propto \epsilon^{1/2}$ .

Fig.4 shows that Eqs.9 and Eqs.11 both give excellent agreement with exact numerics. In the double-resonant case, the cooling is stronger and increases with increasing  $\epsilon$ . In contrast, the single-resonant cooling  $\Gamma_{SR} \propto 1/\epsilon$  and this cannot be improved by increasing  $\epsilon$ . Self-trapping cooling cannot be considered simply in terms of an additive contribution from two intracavity intensities in Eq.6; the response of  $\omega_M$  to the driving is also important. In the double-resonant case,  $\omega_M \propto \epsilon^{1/2}$  for strong driving. In contrast, for the single-resonant case  $\omega_M \propto \epsilon$  and strong driving pushes the  $r2$  resonance into the far-detuned regime. A study of the quantum cooling shows that the minimum phonon numbers attainable  $\bar{n}_{min} \ll 1$  for single and double resonant cooling for strong driving  $\epsilon^2 \gg 1$ . For weak driving, strong cooling can be obtained with single field cooling, but at the edge of the resolved sideband regime  $\omega_M = \kappa/2$ , less favourable for ground state cooling.

*Conclusion* Our study shows that the two-mode self-trapping regime has a raft of of unexpected features, including the split side-bands, strong cooling at blue-detuning and simultaneous heating and cooling resonances. Although other proposals also permit strong cooling rates, the multiple sidebands provide an exceptionally broad region of strong cooling, offering considerable robustness to experimental errors in the driving power, detunings and even the phase (a variation of  $\phi$  of order 30% will not appreciably perturb the strong cooling).

[1] F. Marquardt and S Girvin, Physics **2** 40 (2009).

[2] T. Kippenberg and K. Vahala, Science, **321** 1172 (2008).

[3] C.H. Metzger and K. Karrai, Nature, **432** 1002 (2004).

[4] O. Arcizet et al, Nature, **444** 71 (2006).

[5] S. Gigan et al, Nature, **444** 67 (2006).

[6] C.A. Regal et al, Nature Phys, **4** 555 (2008).

[7] J.D.Thompson et al, Nature, **452** 72 (2008); A.M. Jayich et al New J. Phys, **10**, 095008 (2008).

- [8] A. Schliesser et al, *Nature Physics*, **5** 509 (2009).  
 [9] A. Naik et al, *Nature* **443** 193 (2006); A.D. Armour et al *Phys.Rev.Lett* **88** 148301 (2002).  
 [10] V.B. Braginski and F.Y. Khalili *Quantum Measurement*, Cambridge University Press, 1992.  
 [11] M. Paternostro et al, *New J. Phys.*, **8**, 107 (2006).  
 [12] F. Marquardt et al, *Phys.Rev.Lett* **99** 093902 (2007).  
 [13] I. Wilson-Rae et al, *Phys.Rev.Lett* **99** 093901 (2007).  
 [14] O. Romero-Isart, M.L.Juan, R.Quidant and J.I.Cirac, *New J. Phys.*, **12**, 033015 (2010).  
 [15] D.E.Chang, C.A.Regal, S.B.Papp, D.J.Wilson, O.Painter, H.J.Kimble and P.Zoller, *Proc.Natl Acad.Sci.USA* **107**, 1005 (2010).  
 [16] P.F.Barker and M.N.Shneider, *Phys.Rev.A* **81** 023826 (2010).  
 [17] Schulze R.J., Genes C. and Ritsch H., *Phys.Rev.A* **81** 063820 (2011).  
 [18] O. Romero-Isart et al, *Phys.Rev.A* **83** 013803 (2011).  
 [19] S. Groblacher et al, *Nature*, **460** 724 (2009).  
 [20] H.Miao et al, *Phys.Rev.A* **78** 063809 (2008); C. Zhao et al *Phys.Rev.Lett* **102** 243902 (2009); A. Mari and J.Eisert, arXiv:1104.0260.

## I. APPENDIX

### A. Minimum phonon number

From quantum perturbation theory we can show that  $R_{n \rightarrow m}$ , the rate of transition from state  $n$  to  $n+1$  is:

$$R_{n \rightarrow n+1} = (n+1) \frac{\epsilon^2 \kappa_A}{\omega_M} (S_1(\omega_M) + S_2(\omega_M)) \quad (12)$$

Similarly:

$$R_{n \rightarrow n-1} = n \frac{\epsilon^2 \kappa_A}{\omega_M} (S_1(-\omega_M) + S_2(-\omega_M)) \quad (13)$$

For  $n \gg 1$ , this gives the cooling rate of (Eq.5). However, with the exact expressions we can also show the equilibrium mean phonon number to be:

$$\bar{n}_{min} = \frac{S_1(-\omega_M) + S_2(-\omega_M)}{S_1(\omega_M) + S_2(\omega_M) - S_1(-\omega_M) - S_2(-\omega_M)} \quad (14)$$

The parameters for strongest cooling do not necessarily yield the minimum phonon numbers, because the rate depends upon the difference between the optical heating and cooling, while the phonon number depends upon the ratio between the two. In Figs.5 and 6 we present colour maps comparing the cooling and minimum phonon numbers for both  $R = 0.5$  and  $R = 1$  respectively. Fig.5 corresponds to the same parameters as Fig.2. It shows the broad strong cooling region corresponding to the three distinct cooling resonances  $r2-$ ,  $r1\pm$  which are only partially resolved. The result is a strong cooling region of about 1MHz width, providing the advantage of a strong

cooling regime  $\Gamma \sim \kappa$  insensitive to experimental detunings. For Fig.6 in contrast, the map has a high degree of symmetry, since the role of the modes is interchangeable; the larger  $R$  means the splitting is larger, so  $r1\pm$  are fully resolved at the double resonance: thus only  $r2-$ ,  $r1-$  contribute to the maximal cooling region. Nevertheless, this is the point where the strongest cooling ( $\Gamma = 0.95\kappa_A$ ) is obtained.

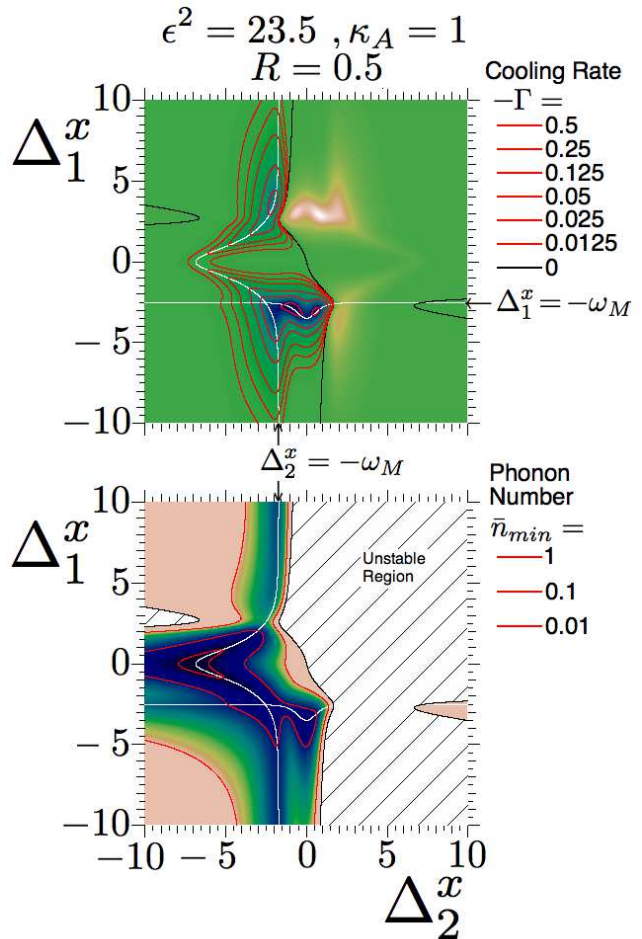


FIG. 5: Colour online) maps of cooling rate and minimum phonon number for parameters  $R = 0.5$  equivalent to Fig.2. The cooling rate map shows information very similar to the shifted curves in Fig.2. The white lines indicate the locus of the single field resonances  $r1\pm$  (where  $\Delta_1^\pm = \omega_M$  and  $r2\pm$ , where  $(\Delta_2^\pm = \omega_M)$ ). Even at the Double Resonance (where the two white lines intersect), there is still a contribution from the partly resolved third sideband of  $r1+$ , giving a very broad strong-cooling region (dark blue). The corresponding broad strong-heating region is also seen for positive  $\Delta_1^\pm$ . *NB*: The axes correspond to corrected detuning scaled to  $A = \kappa$ ,  $\Delta_{1,2}^x$ , not the experimental  $\delta_{1,2}$  of Fig.2.  $R = 0.5$  maximum cooling is  $\Gamma = -0.59$ .

The figures show that the largest cooling rates are found in the symmetric double resonance regime (the double resonance for  $R = 1$ ), the phonon occupancy

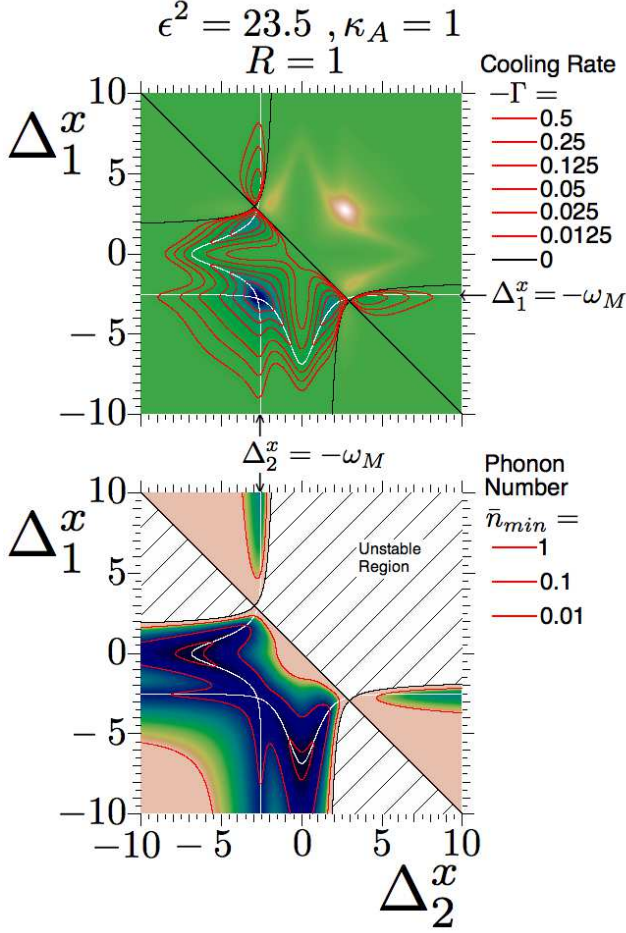


FIG. 6: As for Fig.5 but for  $R = 1$ . The fields are equivalent, thus the cooling/heating maps have a high degree of reflection symmetry. The white lines indicate single field resonance. double resonance occurs where the two white lines intersect. In this case, the splitting between  $r1\pm$  is larger so the double-resonance involves only  $r1-$  and  $r2-$ . The  $R = 1.0$  max cooling is  $\Gamma = -0.95$ ,  $\Delta_1^x = \Delta_2^x = -2.72$ .

is slightly lower in the usually analysed [15] single-field regime where one strong field, at near zero detuning, traps while the other field cools. Nevertheless, the mean equilibrium occupancy is very small in both cases (less than a tenth of a phonon). The above analysis of minimum phonon occupancy has not considered other sources of heating (photon scattering, background gas collisions). The effect of these other heating rates has been analysed in [15] where ground state cooling is shown to be achievable for optimal cooling rates ( $\Gamma \sim \kappa$ ). Thus the 1-2 order of magnitude increase in cooling in the double-resonance region means that this is the most favourable regime.

## B. r2 and single field cooling

The single-field cooling rates are obtained from Eq.5 by taking  $x_0 \simeq 0$ ,  $\Delta_1^x = 0$  and  $\Delta_2^x = -\omega_M$ .

Hence,

$$\Gamma/2 = \frac{\epsilon^2 \kappa_A}{2\omega_M} |\alpha_2|^2 \left[ \frac{1}{[\omega_M - \Delta_2^x]^2 + \kappa_A^2} - \frac{1}{[\omega_M + \Delta_2^x]^2 + \kappa_A^2} \right] \quad (15)$$

We can obtain the precise form given previously [15] if we replace  $|\alpha_2|^2$  using Eq.16:  $\frac{|\alpha_2|^2}{|\alpha_1|^2} \simeq 2x_0 \simeq \frac{\kappa_A^2}{(\Delta_2^x + A/2)^2 + \kappa_A^2}$  and revert to unscaled units.

The above, in principle, requires a full numerical solution of the equations:

$$\alpha_1 = [\kappa_A - i\Delta_1^x]^{-1}; \quad \alpha_2 = R[\kappa_A - i\Delta_2^x]^{-1} \quad (16)$$

$$\tan 2x_0 = |\alpha_2|^2 / |\alpha_1|^2,$$

to find equilibrium positions  $x_0$  and fields. However we can obtain a good approximation in closed form using experimental parameters (driving power, detunings). Hence,

$$\omega_M^2 = \frac{2\epsilon^2}{\kappa_A^2} \quad (17)$$

For resonant cooling  $S_2(-\omega_M) \gg S_2(+\omega_M)$  and cooling/heating by field 1 is negligible. So,

$$-\Gamma \approx \frac{\epsilon^2 |\alpha_2|^2}{\omega_M \kappa_A} \quad (18)$$

and  $|\alpha_2|^2 = \frac{R^2}{\omega_M^2 + \kappa_A^2}$ , hence the Single Resonance (SR) cooling rate becomes:

$$-\Gamma_{SR} \approx \frac{R^2 \epsilon \kappa_A^2}{\sqrt{2}(2\epsilon^2 + \kappa_A^4)} \quad (19)$$

*NB: this is a scaled cooling rate thus given in units of A. This gives a maximum cooling rate if  $\epsilon = \kappa_A^2 / \sqrt{2}$  where*

$$-\Gamma_{SR} \approx \frac{R^2}{4} \quad (20)$$

It is worth noting that this maximum is independent of  $\kappa_A$ : it depends only on  $R$ . (Within the underlying assumption that  $\omega_M \gg \kappa_A$ ) Even for  $R = 1/2$ , the maximum cooling is  $\Gamma_{SR}/2 \sim 1/32$  far from optimal  $\Gamma_{opt}/2 \sim 1$ .

As the driving is increased, if  $2\epsilon^2 \gg \kappa_A^4$ ,

$$-\Gamma_{SR} \sim \frac{R^2 \kappa_A^2}{2\sqrt{2}\epsilon} \propto 1/\epsilon \quad (21)$$

Thus the single resonance cooling rate falls off quite rapidly as the driving amplitude is increased: the optimal cooling cannot be attained by increasing the driving amplitude.

### C. $r2-$ and $r1-$ overlap: double-resonance cooling

As illustrated in Fig.2, the resonances  $r2-$  and  $r1-$  never actually coincide: they undergo something reminiscent of an avoided crossing (recall that Fig.2 is a map of the classical cooling, not of underlying quantum eigenvalues. Nonetheless, the similarity between the classical linearisation and the effective Hamiltonian for the quantum fluctuations has a very similar structure.

The double-field cooling rates for the region of closest approach are estimated from Eq.5 by assuming that the two resonances actually cross, in other words both fields are, to a good approximation, simultaneously resonant.

The first task is to identify the  $\epsilon$ -dependent pair of detunings for which:

$$-\omega_M(\Delta_1, \Delta_2) \approx \Delta_1^x \approx \Delta_2^x \quad (22)$$

One can search numerically for detunings which give near-simultaneous resonances. However, for moderate  $\sin 2x_0 \simeq \tan 2x_0 \simeq 2x_0$ , a closed form can be obtained. Provided  $R$  is small the double resonance still falls in the small angle regime (including our Fig.2). In this case, From Eq.16:

$$2x_0 \simeq R^2 \frac{(\Delta_1^x)^2 + \kappa_A^2}{(\Delta_2^x)^2 + \kappa_A^2} = R^2 \quad (23)$$

so if  $\Delta_1^x = \Delta_2^x = -\omega_M$  we obtain  $x_0 \simeq R^2/2$ .

The mechanical frequency:

$$\omega_M^2 = 2\epsilon^2 |\alpha_1|^2 = \frac{2\epsilon^2}{(\Delta_1^x)^2 + \kappa_A^2} = \frac{2\epsilon^2}{\omega_M^2 + \kappa_A^2} \quad (24)$$

this means:

$$\omega_M^2 = \frac{-\kappa_A^2}{2} + \frac{1}{2} \sqrt{\kappa_A^4 + 8\epsilon^2} \quad (25)$$

In this case, there are contributions to cooling from both field 1 and field 2. Adding them both,

$$-\Gamma_{DR} \approx \frac{\epsilon^2(R^2 + R^4)}{\kappa_A \omega_M (\omega_M^2 + \kappa_A^2)} \quad (26)$$

where we will substitute Eq.25 to evaluate the frequency  $\omega_M$ . As ever,  $\omega_M \gg \kappa_A$ :

$$-\Gamma_{DR} \approx \frac{R^2 \epsilon^{1/2}}{2^{3/4} \kappa_A} \quad (27)$$

Eqs.26 and 27 should be contrasted with the behaviour of the singly resonant cooling Eq.10. In the double-resonant case, the cooling increases, without limit, as a function of  $\epsilon$ . For  $R = 1/2$  and  $\epsilon^2 \simeq 100$  (ie 8mW power),  $\Gamma \simeq 0.4A$ . In Fig.4 the approximate expressions Eqs.10,26,27 are shown to give quite good agreement with cooling rates obtained from numerical solution of the equations of motion, without linearisation.

The very large damping rates provided by the double-resonant regime have the added advantage of relative insensitivity to the initial preparation. Although the analysis assumes small oscillations about equilibrium  $x_0$ , a resonator prepared at the antinode of the trapping field ( $x = 0$ ) is very rapidly pulled towards equilibrium and oscillates about  $x = x_0$ . Consequently there is no need to provide any initial displacement. In addition, the multiple resonance region shown in Fig.2 is surprisingly robust to errors in the relative phase between the two modes. In Fig.5 we see that a phase error of order 20% makes relatively little difference (and may even enhance the cooling).

### D. Symmetric double-resonance cooling

The best regime for strong cooling is one in which the fields are equally strong and where both are resonantly, red detuned. In this region:

$$\omega_M = \sqrt{\frac{-\kappa_A^2}{2} + \sqrt{\frac{\kappa_A^4}{4} + 2\sqrt{2}\epsilon^2}} \quad (28)$$

and:

$$\Gamma_{opt} = \frac{\epsilon^2 \kappa_A}{\omega_M} \frac{1}{\kappa_A^2 + \omega_M^2} \left( \frac{1}{\kappa_A^2} - \frac{1}{\kappa_A^2 + 4\omega_M^2} \right) \quad (29)$$

In the limit  $\omega_M \gg \kappa_A$ :

$$\Gamma_{opt} = \frac{2^{-9/8} \sqrt{\epsilon}}{\omega_M} \quad (30)$$

This is not simply a special case of Eq.27 because we have moved away from small  $x_0$  into the regime  $x_0 = \pi/8$ . However the difference between Eq.27 and the above is less than a factor of 2.

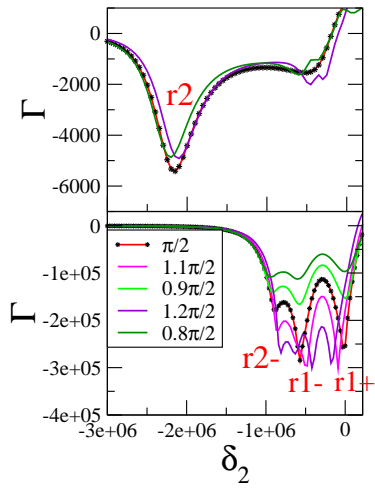


FIG. 7: Shows that the strong cooling region where the split sidebands  $r2-$ ,  $r1-$ ,  $r1+$  overlap is reasonably insensitive to the phase difference between the two modes. A variation of about 30% about the usual dephasing of  $\pi/2$  is tolerable (and can even give enhanced cooling).